



CrossMark
 click for updates

Cite this: *RSC Adv.*, 2016, 6, 104782

Acid-catalyzed oligomerization *via* activated proton transfer to aromatic and unsaturated monomers in Nafion membranes: a step forward in the *in situ* synthesis of conjugated composite membranes†

Sagar Motilal Jain,^{*adf} Sapana Tripathi,^b Sanjay Tripathi,^c Giuseppe Spoto^d and Tomas Edvinsson^{*e}

An approach to perform controlled acid-catalyzed oligomerization *via* vapor pressure control of the reactions inside Nafion membranes is presented. The interaction of Nafion with several classes of aromatic (pyrrol, furan, thiophene) and unsaturated (methyl-acetylene) gas phase monomers was studied as a function of contact time and temperature by *in situ* vibrational (FTIR) and electronic (UV-Vis) spectroscopy with the support from theoretical linear response and time dependent DFT calculations to monitor the vibrations and the effective number of conjugated double bonds. The formation of H-bonded adduct as seen from IR spectroscopy transforms the hydrogen bonded species into positively charged oligomers through an activated proton transfer mechanism where oligomerization progress through increasing contact time with the respective gas phase reactants at room temperature. The activated proton transfer oligomerization proceeds through the stepwise growth propagation cycles *via* carbocationic intermediates, finally leads to the formation of irreversible, conjugated charged oligomers as a product. The colored, conjugated oligomeric Nafion composite products are formed at room temperature as a function of reaction time and are irreversible after complete degassing of the gas phase reactants as well stable in ambient environment stored for many days in pure oxygen or air and cannot be extracted with common solvents, appearing strongly encapsulated inside Nafion membranes. This is crucial for future applications of the presented route for direct production of conjugated species inside Nafion and thus production and control of composite membrane materials of interest in fuel cells and catalysis.

Received 16th September 2016
 Accepted 24th October 2016

DOI: 10.1039/c6ra23105e

www.rsc.org/advances

Introduction

Conductive polymeric membranes are widely used as a key component of solid electrolyte membrane fuel cells (PEMFC) and are expected to be an important part of the near future

technologies of clean energy for transportation, stationary and portable applications. Among the conductive polymeric membranes available for clean energy application, Nafion membranes are extensively studied^{1–10} as they represent the most effective membranes for proton conductivity in devices operating in the 60–80 °C temperature range, although they suffer from some drawbacks like low chemical and thermal stability, high permeability to methanol and other fuels, and strong dependence of the proton conductivity on the humidity.^{6–10} Hybridization with other materials represents a promising route to solve some of these problems. It has been for instance reported that incorporation of sulfonated single-walled carbon nanotubes⁶ or graphene¹¹ improves the Nafion proton conductivity as well as the chemical and mechanical properties. Increased separation of charge carriers and decreased methanol cross-over on hybridization with polypyrrole,^{12–14} improved mechanical stability and modified water uptake with imidazole and poly benzimidazole^{15,16} have also been reported as well as improved stability in vinylimidazole

^aUppsala University, Department of Chemistry – Ångström Laboratory, Physical Chemistry, Box 523, SE 751 20 Uppsala, Sweden. E-mail: sagarmjain@gmail.com

^bMax Planck Institute for Intelligent Systems, Department Magnetic Materials, Heisenbergstraße 3, 70569 Stuttgart, Germany

^cMahakal Institute of Technology and Management, Dept. of Mechanical Engineering, Behind Air Strip, Datana, Dewas Road, 456664 Ujjain, M.P, India

^dDepartment of Chemistry, NIS (Nanostructured Interfaces and Surfaces) Centre of Excellence, University of Torino, Via P. Giuria, 7, 10125 Torino, Italy

^eDepartment of Engineering Sciences – Solid State Physics, Uppsala University, Box 534, SE 751 21 Uppsala, Sweden. E-mail: tomas.edvinsson@angstrom.uu.se

^fCollege of Engineering, Swansea University Bay Campus, Fabian Way, SA1 8EN Swansea, UK

† Electronic supplementary information (ESI) available: Additional FTIR and UV-Vis spectra. See DOI: 10.1039/c6ra23105e

hybridized Nafion¹⁷ where Nafion serve as a macroinitiator for radical polymerization. However, the improved properties are closely related to the membrane structure and morphology which in turn is dependent on the type of molecule and nature of oligomerization state of the hybridized materials and has so far been difficult to control. There is thus a strong need to be able to both control and understand the hybridization process and mechanism for different classes of molecules in order to both control and fine-tune the benign properties without introducing undesired properties. The polymerization can be performed *in situ* due to the strong Brønsted acidity properties of Nafion where a detailed knowledge of the polymerization mechanism is vital to control the process and finally fine-tune the physical–chemical properties of the resulting hybrid membrane. The super acid, Nafion-H is a known polymerization catalyst; isobutylene has been polymerized with Nafion-H resulting in the formation of oligomers also with higher alkenes *viz.* 1-decene (at 120 °C), and the oligomerization of styrene has previously been performed using Nafion as a catalyst by Higashimura and co-workers.¹⁸

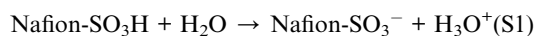
Here we investigate the acid-catalyzed polymerization of a variety of aromatic heterocyclic (pyrrole, thiophene and furan) as well unsaturated (methyl-acetylene) monomers inside Nafion by *in situ* IR and UV-Vis spectroscopies collaborated with DFT calculations for mechanistic investigations of the oligomerization mechanisms.

Infrared spectroscopy is a highly sensitive tool to monitor proton transfer reactions and thus suitable to distinguish Nafion in protonated and deprotonated states (ESI Fig. S1†) and further to monitor the proton transfer when polymerization occurs.¹⁹ The different steps in the oligomerization process are followed by UV-visible, FTIR spectroscopies and compared with theoretical linear response and time dependent DFT calculations to monitor the vibrations and the effective number of conjugated double bonds, hence probed the main polymerization products formed in the HTO oligomerization process.

Results and discussion

Spectroscopy of protonated and deprotonated Nafion membrane

To perform the detailed IR and UV-visible investigation on the acidic Nafion membrane, the infrared as well electronic spectral differences in protonated (hydrated) and deprotonated (dehydrated) states during proton transfer are important to understand. Monitoring the transformation of dehydrated to hydrated Nafion with IR and UV-visible spectroscopy evidence a proton transfer reaction as:



Proton transfer is also reported before by Buzzoni *et al.*²⁰ and also here we experimentally probed and discussed in detail, ESI Fig. S1.†

In Fig. 1(a), an overview of the Nafion structure, the hybridizational species and a Nafion channel where an initial

oligomerization step with activated proton transfer is illustrated. To support the experimental findings and the identification of the intermediate critical adducts we have performed linear response DFT and TD-DFT to obtain theoretical IR and UV-Vis transitions illustrated in Fig. 1(b) and (c).

Oligomerization of heterocyclic aromatic compounds: pyrrole, furan and thiophene in Nafion

Membrane

FTIR – vibrational spectroscopy of aromatic/Nafion system. Polypyrrole has previously been reported to be synthesized through oxidative polymerization, using various organic oxidizing agents or by electrochemical methods.^{20–23} However, this approach yield a loss in conjugation and thus impede conductivity. There are also some approaches in this direction in the patent literature which contains a report of cationic polymerization of tetrahydrofuran (THF) in Nafion.²⁰

To the best of our knowledge, the route to polymerize several different classes of organic compounds with a room temperature proton activated precursor in Nafion has not been reported before. Below we analyze this route using methyl acetylene, pyrrole, furan and thiophene polymerization exploiting the Brønsted acidity of Nafion with the important result of a preservation of the conjugation of the final oligomeric products. Understanding the features of the IR spectra of protonated species (acidic Nafion), is complicated as reported by Buzzoni and co-workers.²⁰ The experimental vibrational spectrum of a concentrated solution of Nafion and hybridization oligomers can also be challenging to analyze, especially where individual bands can be suppressed or broadened by the interaction. To this end, we have added linear response DFT calculations for assignment of the IR bands of the Nafion *per se* and the vibrations of the conjugating bonds in-between the monomers without interaction by analyzing the displacement vectors of the vibrational modes where shifts and broadening would give some additional information of possible interactions. A prototypical Nafion polymer is used in the calculations with 9 carbon and 2 oxygen atoms in the back bone chain and terminated with a sulfonate group. We have also included one branch point to be able to distinguish back bone bending and vibrations that occur over the branch point in comparison to the “linear” part of the Nafion chain. The Nafion polymer is depicted in the inset of Fig. 2 which show the theoretical IR spectrum calculated on a B3LYP/6-311G(d,p) level using Gaussian09.²¹ The back bone bending *via* C–C and C–O stretching indeed show a split of vibrations when occurring in the linear part of the chain (assignment 3, 906 cm⁻¹) or when occurring over the branched point (assignment 4, 982 cm⁻¹). Assignments important for the experimental parts are the S–O stretching (assignment 2, 773 cm⁻¹) and the S=O stretching (assignment 9, 1404 cm⁻¹). Other theoretical assignments for the major bands can be found in Table 1. The major change in the IR spectrum upon deprotonation in Nafion comes from the transformation from a low symmetric –SO₃H subgroup (C₁ symmetry) with strong S–O vibration to a symmetric –SO₃ subgroup (C_{3v}) with strong

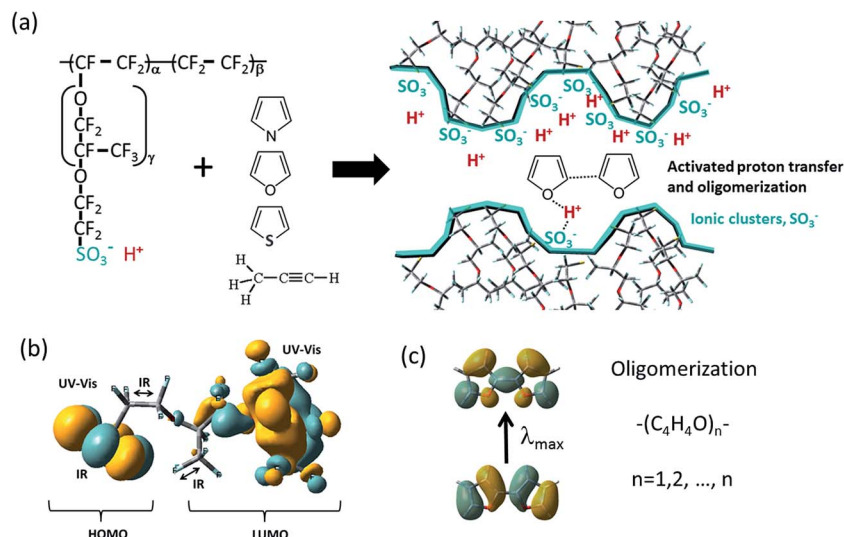


Fig. 1 (a) The chemical structure of Nafion and the aromatic and unsaturated monomers investigated in this study together with an illustration of an activated proton transfer in a Nafion channel during an oligomerization step for the formation of the furan dimer. (b) The HOMO and LUMO frontier orbitals of a deprotonated Nafion polymer as calculated on a 6-311G(d,p) level with B3LYP and schematic depiction of some of the vibrational modes probed with IR and linear response DFT in this study. (c) The frontier orbitals for the lowest excitation energy transition (λ_{\max}) for a furan dimer where the theoretical values for oligomerization up to 5 units for pyrrole/furan/thiophene can be found in Table 3.

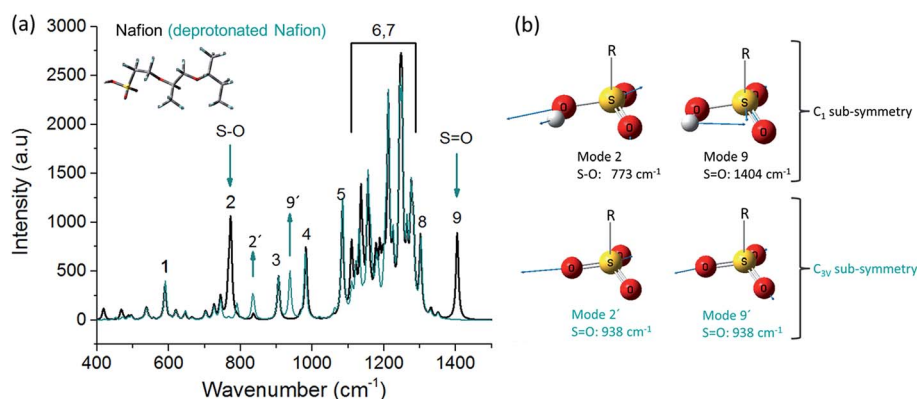


Fig. 2 (a) Theoretical IR spectra of a branched Nafion molecule (black line) deprotonated branched Nafion (green line) calculated on a B3LYP/6-311G(d,p) level. The green arrows indicate the modes with the largest differences between protonated and deprotonated Nafion and the numbers are the assignments summarized in Table 1. (b) Sub-symmetry modes and shift in frequencies in the sulfur oxygen bonds when deprotonated.

S=O vibration as seen in Fig. 2 and was also reported in a recent study on the IR spectra of hydrated and dehydrated Nafion in the context of ion-exchange in Nafion membranes.²⁵ Additionally we have performed theoretical IR on the same level of theory for the pure sulphonic acid, H₂SO₄, to be able to distinguish contributions from possible sulphonic acid species. Here we find two modes at (768, 830 cm⁻¹) for symmetric S-O and asymmetric S-O and (1193, 1402 cm⁻¹) for symmetric S=O and asymmetric S=O respectively. HSO₄⁻ gave 701 cm⁻¹ for S-O stretch while the three S=O bonds showed one symmetric S=O at 1007 cm⁻¹ and three asymmetric stretches at 1124, 1214, and 1268 cm⁻¹. SO₄²⁻ with high symmetry and essentially the same bond lengths for equally distributed electrons gave IR vibrations at 1060–1063 cm⁻¹.

Here the relevant bands for the experimental parts are bands at around 1060 cm⁻¹ for SO₄²⁻ and the asymmetric S=O stretch in HSO₄⁻ at around 1400 cm⁻¹.

We can also follow the oligomerization process of the aromatic monomers in the system by analyzing the IR response of the C-C bond created in between the monomers. This bond vibration intensity is in the deprotonated system very weak due to that the dipole is perpendicular to the bond as seen in Table 2, while the protonation in the proton activated step breaks this symmetry and introduce an electron density anisotropy. This changes the possibilities for nucleophilic and electrophilic attack as well as strongly enhance the dipole change and thus the IR intensity during the C-C vibration connecting the monomers in the oligomerization process.

Table 1 Assignment of major modes in Nafion, $\text{CF}_3\text{-(CF}_2\text{-O-CF}_2\text{)-CF}_3\text{-SO}_3\text{H}$, in the theoretical IR spectra calculated with DFT on a B3LYP/6-311G(d,p) level with assignment numbers from IR spectra in Fig. 1

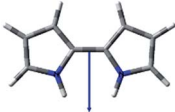
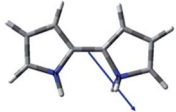
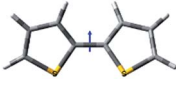
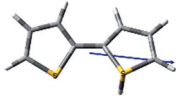
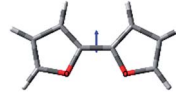
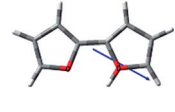
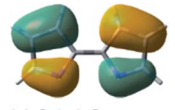
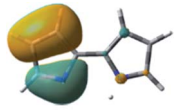
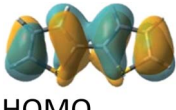
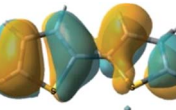
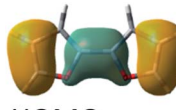
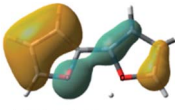
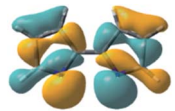
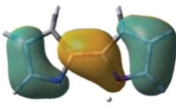
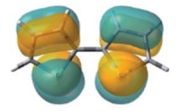
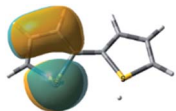
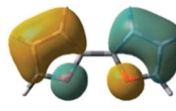
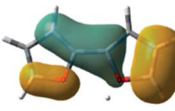
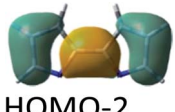
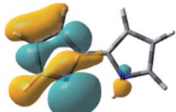
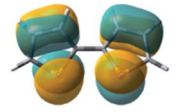
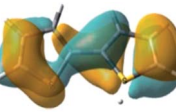
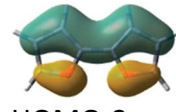
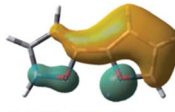
Assignment number	Band (cm^{-1})	Assignment
1	590	Symmetric S-O bend combined with S-C stretch
2	773	S-O
3	906	Backbone bending <i>via</i> C-C and C-O stretch
4	982	Backbone bending <i>via</i> C-C and C-O stretch over a branched part of Nafion
5	1084	C-O
6	1110–1210	C-O, C-C combination modes
7	1220–1300	C-C combination modes with small C-O contribution
8	1302	C-C
9	1404	S=O
Not shown	3760	O-H

The characteristic bands of these vibrations between 1500 and 1700 cm^{-1} are not hidden by IR bands from either Nafion or the protonated Nafion (see Table 1 and Fig. 2) and allow

identification of both the creation of bonds in between the monomers as well as from their high intensity, that the symmetry of the dipoles in the oligomers are broken by protonation as seen in Table 2. Successive oligomerization introduces more connecting C-C bonds and combination modes and thus broadens the IR bands. The exact extent of oligomerization is difficult to quantify with IR since the intensity and broadening of the polymerization bond is also sensitive to the hydrogen bonding environment and is later instead analyzed in terms of the effective conjugation length as given from the optical response. With this in mind we can now analyze the experimental IR spectra in more detail.

Fig. 3(a)–(f) show the FTIR spectra of pyrrol/Nafion, furan/Nafion and thiophene/Nafion composites respectively. In the low frequency part of the IR spectra of $(\text{CF}_3)_n\text{-SO}_3\text{H}$ (Fig. 3(b), (d) and (f) spectrum number 1), the S=O stretching mode observed at 1413 cm^{-1} ,^{20,25–27} while the modes with prevailing S-OH character are started appearing at 913–983 cm^{-1} (Fig. 3(b), (d) and (f) spectrum number 1) gradually increasing. Similar to that of the spectrum previously reported for sulphuric acid.²⁷ In the spectrum, Nafion bands from HSO_4^- and SO_4^- species are observed at 1414 and 1050 cm^{-1} respectively (found at 1402 and 1060 cm^{-1} for gas phase species in the theoretical and experimental IR).

Table 2 DFT optimized ground state structures and dipoles of the aromatic dimers and protonated dimers. The three highest bonding orbitals and the major IR mode and relative intensity for the C-C bond in between the monomers for the dimers and protonated dimers calculated with linear response DFT from the ground state structures on a B3LYP/6-311G(d,p) level

Pyrrole	Pyrrole-H ⁺	Thiophene	Thiophene-H ⁺	Furan	Furan-H ⁺
					
$\mu = 3.16$ D	$\mu = 5.53$ D	$\mu = 0.99$ D	$\mu = 4.24$ D	$\mu = 1.00$ D	$\mu = 3.25$ D
					
HOMO	HOMO	HOMO	HOMO	HOMO	HOMO
					
HOMO-1	HOMO-1	HOMO-1	HOMO-1	HOMO-1	HOMO-1
					
HOMO-2	HOMO-2	HOMO-2	HOMO-2	HOMO-2	HOMO-2
Dimer C-C IR mode NA Relative IR intensity 0	Dimer C-C IR mode 1677 cm^{-1} Relative IR intensity 470	Dimer C-C IR mode 1484 cm^{-1} Relative IR intensity 22	Dimer C-C IR mode 1629 cm^{-1} Relative IR intensity 251	Dimer C-C IR mode 1539 cm^{-1} Relative IR intensity 45	Dimer C-C IR mode 1703 cm^{-1} Relative IR intensity 483

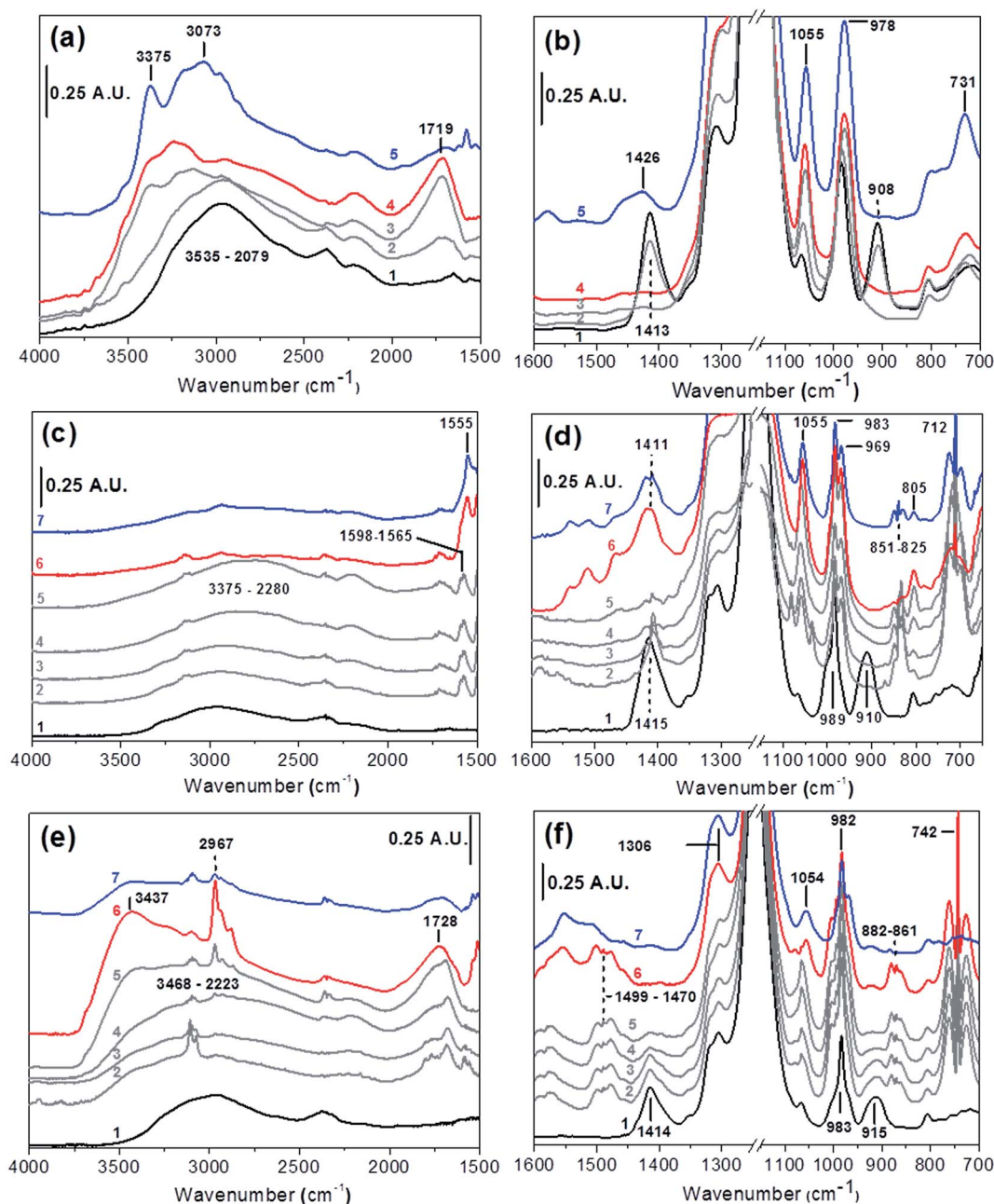
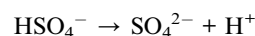


Fig. 3 FTIR spectroscopy of aromatic/Nafion composite: (a), (b) pyrrol/Nafion composite; (c), (d) furan/Nafion composite and (e), (f) thiophene/Nafion composite. Black spectrum number 1 is H-Nafion degassed at 100 °C for 30 minutes. Grey spectra (spectrum number 2 and onwards) represents the effect of increasing the contact time (about 2 minutes interval for each spectrum, except for pyrrol/Nafion system where the first changes in FTIR were registered after ~20 min reaction time) after a dosage of respective gas monomers on Nafion membranes at room temperature; red spectra represents aromatic/Nafion system after annealing in presence of excess respective monomer reactants at 100 °C for 30 minutes. The spectra marked in blue are IR after degassing respective gas phase monomer reactants. Decreasing bands correspond to species which are consumed upon aromatic heterocyclic monomer dosage. While the positive/increasing bands correspond to species which are formed.

The band at 1050–1054 cm^{-1} is due to SO_4^- vibrations growing at the expense of the HSO_4^- band at 1414–1416 cm^{-1} after dosing of pyrrol, furan and thiophene followed by regular interval of time (Fig. 3(b), (d) and (f) grey spectra). Thus the band due to HSO_4^- (1414 cm^{-1}) is completely eroded and there is formation of new band of SO_4^- (1050 cm^{-1}). The changes in the FTIR spectrum are clear indications of the protonation²⁰ reaction:



While these changes happening in fingerprint region, the higher wavenumber at the same time show broad and complex spectra (Fig. 3(a), (c) and (e)) associated with interaction with protonated $\text{H}_{2n+1}\text{O}_{n+}$ species (broad bands at 2700, 1750 and

1200 cm^{-1}). The increasing intensity of a strong peak at ~ 1056 (Fig. 3(b) spectra 2, 3 and 4), ~ 1055 (Fig. 3(d) spectra 2, 3) and 1065 cm^{-1} (Fig. 3(f) spectra 2, 3) is increasing with time evolution in contact with pyrrole, furan and thiophene gas phase respectively, at room temperature can consequently be assumed as the fingerprint of the proton transfer from undissociated acid to water.

At room temperature with increased reaction time with respective aromatic heterocycles, the broad absorptions in the 1800–1600 cm^{-1} intervals are well distinguishable in the spectrum (Fig. 3 spectra (a), (c) and (e)) and are due to inner internal and external groups (*i.e.*, those more directly linked to the proton (H^+) and whose bending frequency is, as expected, upward shifted because they are involved in stronger hydrogen bonding).²³ IR bands in the range of 1413, 1055, 981 and 961 cm^{-1} are related to C–C bond vibrations^{30,31} and are assigned in more detail here *via* DFT calculations and the assignments of the vibrations in the Nafion membrane in Table 1. As far as the second absorption in the 1350–850 cm^{-1} (Fig. 3(b), (d) and (f) grey spectra) interval is concerned, it is associated with the second bending mode of internal and external C–C and C–O groups (also possibly upward shifted with respect to normal vibrations because of the stronger interactions in a bonded Nafion membrane). Note, that also the stretching vibrations of strongly hydrogen bonded OH groups have been suggested to contribute in this region.¹⁹

The electrophilic attack of the strong Brønsted groups on the weakly adsorbed precursors and successive oligomerization reveal an activated process which can be followed by FTIR, as illustrated in Fig. 3 and further motivated by the anisotropic charge distribution of the protonated species and thus strongly enhanced IR activity of the C–C bond in between the monomers as seen in DFT results in Table 2. Evolving with time, one can notice that the intensity of the peaks at 3451 cm^{-1} due to $\nu(\text{NH})$, at 3141 and 3116 cm^{-1} due to $\nu(\text{CH})$, and at 1531, 1469, 1419 and 1378 cm^{-1} due to the ring stretch modes of the weakly adsorbed precursors gradually decrease, while the bands attributed to the acid catalyzed transformation product (products) of pyrrole, furan and thiophene increases (especially the absorption in the ~ 3300 – 2300 cm^{-1} interval and the band at ~ 1450 – 1460 cm^{-1}).²⁸ The thermal treatments at 100 °C, 30 minutes for the pyrrole/Nafion, furan/Nafion and thiophene/Nafion systems were performed *in situ* in the presence of an excess gas phase pyrrole, furan and thiophene respectively.

The evolution of the IR spectrum of the pyrrole/Nafion system with the temperature (Fig. 3 red spectrum) show that the intensity of the bands in 1300–1500 cm^{-1} interval can be assigned to monomeric (protonated) species and the bands due to weakly adsorbed pyrrole (Fig. 3(b) spectrum 3), furan (Fig. 3(d) spectrum 5) and thiophene (Fig. 3(f) spectrum 5) at room temperature decrease when the temperature is increased and that new species are simultaneously formed characterized by bands at 1621, 1521, 1485, 1452, 1431, 1377 and 1344 cm^{-1} . For the furan/Nafion system the assignment of the IR bands is essentially the same given the liquid and gas phase spectra (ESI Fig. S3†) and consequently does not need a specific comments. Nevertheless, a few considerations on a selected number of IR

bands will be made in the following to facilitate comparison with the spectra of thiophene on Nafion.^{28,29} In the case of polythiophene (PTh) there is significant band in 1334 cm^{-1} related to the C=S bond.³⁰ Which in our case is reduced and shifted to lower wave number by a factor of $d_\nu = -30 \text{ cm}^{-1}$, this can be due to H-bonding effect as well as due to overlapping by the high C–C bonds. The shift is also consistent with our DFT calculations showing this band at around 1260 cm^{-1} for the protonated dimer and is expected to be broadened and shifted with further oligomerization. Bands seen at 981, 966, 841, 803 cm^{-1} are due to the C–H bends in thiophene ring.³¹ This is further confirmed from our linear response DFT where we can assign the vibrations in the lower part of 800 cm^{-1} to asymmetric C–H bends but also see a clear C–S vibration at 860 cm^{-1} that couple to symmetric C–H bending seen at 841 cm^{-1} in the calculations.

For the thiophene/Nafion system (Fig. 3(e) and (f)) after dosing thiophene a band is visible in the 790–700 cm^{-1} due to the out of plane bending of $\delta(\text{CH})$ of thiophene in gas phase (with typical rotovibrational profile), as well absorptions at 887–850 cm^{-1} deformation mode outside the ring plane. On increasing the contact time with the gas, the disappearance of the bands of the ionized sulphonic 1410 cm^{-1} stretching modes of $\nu(\text{S}=\text{O})$ and 910 cm^{-1} stretching modes of $\nu(\text{S}-\text{OH})$ is seen and an increase in intensity of the band at 1060 cm^{-1} species dissociated SO_3^- (Fig. 3(e) and (f)). In addition new bands appear in the region 1757–1623 cm^{-1} , after heating thiophene/Nafion system (Fig. 3(e) and (f) spectrum 6). Alike that of furan/Nafion system (Fig. 3(c) and (d) spectrum 6).

For the aromatic/Nafion system, the evolution of spectrum in the 3500–2500 cm^{-1} range (Fig. 3 curves (a), (c), and (e)) is less informative, since the bands becomes broader and form a nearly structure-less envelope. All the data suggests that an increase of temperature favors the formation of new structures at the expense of the monomeric species (both neutral and positively charged). This is further investigated with ultraviolet-visible (UV-visible) spectroscopy.

The reaction products formed of the aromatic/Nafion composite at room temperature are irreversible, so the obvious expectation validates the irreversibility of product formed after 100 °C. This is verified by outgassing the gas phase reactants where the bands belongs to the oligomeric products remains unaffected with only the disappearance of gas phase reactants (Fig. 3 blue spectrums). This is an important observation as it reveals an irreversible chemical interaction and encapsulation of the product inside the Nafion matrix. This is also supported by calculations of the dimerization process with DFT with a furan and a protonated furan monomer which shows a clear lowering of the energy upon bond formation also without any stabilization with external surrounding or other species.

UV-visible – electronic spectroscopy of heterocyclic aromatic/Nafion system. FTIR spectroscopy shows the proton transfer and formation of oligomer products. But the separate contributions in IR spectra from each species in the hybrid materials become broadened and difficult to interpret. In a more practical situation, it is also desirable to control the extent of

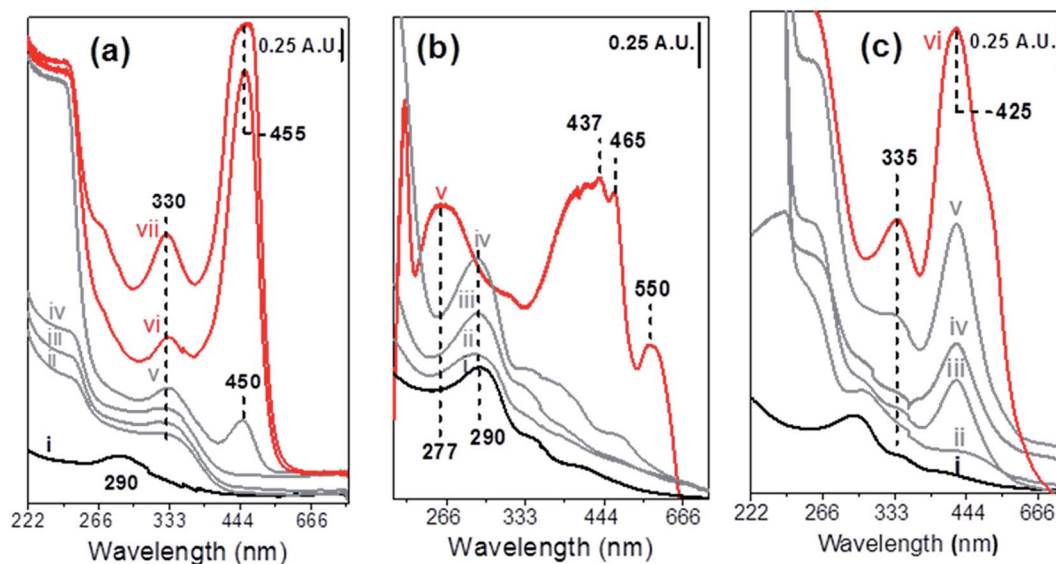


Fig. 4 UV-visible spectroscopy of aromatic/Nafion composites: (a) pyrrole/Nafion composite, (b) furan/Nafion composite, (c) thiophene/Nafion composite. Black (spectra i) is H-Nafion degassed at 100 °C for 30 minutes. Grey spectra (spectrum ii and onwards) represents the effect of increasing contact time (about 2 minutes interval for each spectrum, except for pyrrol/Nafion the first spectrum registered after 20 min reaction time and other spectrum after the subsequent interval of ca. 40 min each) after a dosage of respective gas monomers on Nafion membrane at room temperature; red spectra represents respective aromatic/Nafion system after annealing in presence of excess of respective monomer reactants at 100 °C for 30 minutes. In case of pyrrole/Nafion composite (a) spectra v, represent the pyrrole/Nafion system after 180 min of contact time at room temperature; spectra vi and vii represent the sequential heating at 100 °C for 10 and 30 minutes respectively.

oligomerization in simpler ways where the color of the hybridization products is a marker of the effective conjugation length. Therefore UV-visible spectroscopy is employed to analyze the colored oligomeric products formed where the number of effective conjugated double bonds in the products can be probed by comparing with experimental and theoretical data for the optical transitions for different conjugation lengths.

The dependence of the UV-visible spectrum of the aromatic/Nafion system as a function of reaction time and temperature is shown in Fig. 4.

We can notice that shortly (2 minutes reaction time, except for pyrrol/Nafion system where the first spectrum with significant change is after ~20 minutes of reaction time) after dosage of reactant gas species for aromatic/Nafion systems, dosage at their respective vapor pressure shows the change in UV-visible spectrum a noticeable absorption appears in the visible region of the spectrum centered at ca. 330 nm, 290 nm and 425 nm respectively for pyrrol/Nafion, furan/Nafion and thiophene/Nafion systems (Fig. 4(a)–(c)). The absorption of furan/Nafion system to a relatively shorter wavelength is due to the fact that unlike pyrrole and thiophene the furan has a lower conjugation due to lower p orbital extension of oxygen compared to that of nitrogen and sulfur.

On increasing the reaction or contact time of Nafion with the respective gas phase of aromatic monomers, at room temperature this absorption grows in intensity progressively shifting to 450 nm (after 60 min of reaction time) for pyrrol/Nafion system and shifting to ~388 nm and broad absorption centered 480 nm from 290 nm for furan/Nafion system (Fig. 4(b)). For thiophene/Nafion system the UV-Vis shift from 295 nm to remarkable

absorption at 444 nm. This observation of further red shift in visible region with increased intensity for all aromatic/Nafion system reflects the change in color of the Nafion membrane from transparent (Nafion) to orange brown (aromatic/Nafion composite) as shown in Fig. 5 for pyrrol/Nafion composite.

Although initially the reaction is slow for pyrrol/Nafion system, after long contact of about 180 min (in presence of excess pyrrol) the reaction proceeds giving rise to intense brown color to the membrane.

Further heating at 100 °C for 30 min for pyrrol/Nafion as well for furan/Nafion system shows intensified UV-Vis absorption as an indication of formation of increased number of conjugated double bonds. For furan/Nafion system the significant red shift down to the limit of visible region 437–465 and 550 nm and increase in intensity (increase in number of conjugated double bonds) are observed after heat treatment at 100 °C for 30 min.

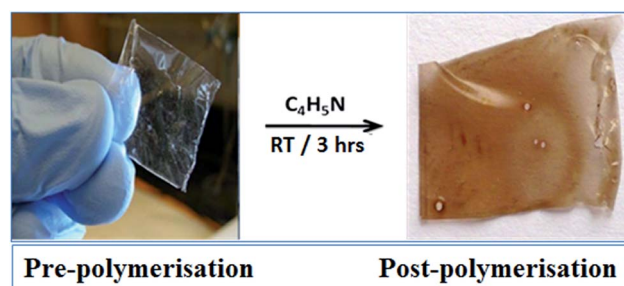


Fig. 5 The picture illustrates color change of Nafion membrane at room temperature after in contact with gas phase pyrrol for 3 hours of reaction time.

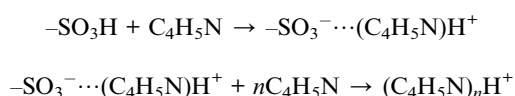
However, thiophene/Nafion system do not show any red shift but only increased intensity, absorbance on heating as an indication of saturation point of formation of the conjugated oligomeric products at room temperature.

From above observation it is clear that the oligomerization of different aromatic monomers proceed with different speed as provided the functionality of the reactant monomers the speed of reaction for aromatic monomer is in order: thiophene > furan > pyrrol. The reason of the different reaction rates can be rationalized by the DFT optimized ground state structures and dipoles of the aromatic dimers and protonated dimers Table 2. And is further discussed below.

Although variable speed of reaction of above aromatic monomers with Nafion membrane, some common observation can be put forth as for aromatic/Nafion UV-Vis and FTIR spectroscopy shows consistent formation of di, tri and tetra-oligomeric carbocationic structures containing number of conjugated double bonds varying from three (330 nm) to six (555 nm).^{24,32}

For aromatic/Nafion system the appearance and increasing intensity of the band at 230 nm with increasing reaction time (aging effect) could be due to a chromophore generated by a fluorocarbon radical as well as loss of H₂O. The decreasing degree of hydration increases the interactions among the auxochromic group and the chromophore shifting, and increases the absorption intensity of the band in the region of ~200 nm. The bands at 350 nm and 400 nm is associated with the chromophore of a *SO₃H radical. This last radical cleaves to produce SO₂ and a hydroxyl radical.³³ The chromophore responsible for absorptions at 350 nm and 400 nm are more uncertain but can probably be associated with a sulphur-based groups.

The IR spectral signatures observed in Fig. 3(a) and (b), the UV-Vis in Fig. 4(a), and the theoretical data in Table 3 then comply with formation of the pyrrol/Nafion oligomers as summarized in the following reaction steps:



where $n = 3-5$.

For the thiophene/Nafion composites, immediately after dosage of the thiophene gas phase, a new shoulder peak appears at around 420 nm and accompanied by the disappearance of the band at 290 nm (Fig. 4(c) spectrum ii) that corresponds to the thiophene dimers by comparing with the time dependent DFT results in Table 3. As the contact time increases (spectra iii to v), new absorption gradually develops and centered around 277 nm and 437 nm (broad), and 550 nm (weak) (spectrum v). The experimental UV-visible spectra here shows good agreement with previous analysis of optical spectra of corresponding oligomers³³ and cross-reference therein of the thiophene/H-Y Zeolite system as well as strongly supported by the time-dependent DFT data of the optical transitions in Table 3. Based on this it is possible to assign the broad band around 437 nm as protonated monomer C₄H₅S⁺ or possibly a partially protonated dimer, C₄H₄S-H-SH₄C₄⁺. To be able to distinguish

Table 3 First excited state optical transitions with high oscillator strength of the different oligomers from TD-DFT performed at B3LYP/6-311G(d,p) level in the gas phase

Structure	Oligomer	Transition λ_{max} (nm)	Oscillator strength
Pyrrole	Mono	260	0.01
	Di	296	0.74
	Tri	417	0.48
	Tetra	513/554	0.53/0.19
	Penta	709/683	0.17/0.25
Thiophene	Mono	211	0.09
	Di	293	0.37
	Tri	353	0.68
	Tetra	415	1.10
	Penta	487	1.55
Furan	Mono	194	0.15
	Di	275	0.59
	Tri	337	0.87
	Tetra	386	1.23
	Penta	428	1.27

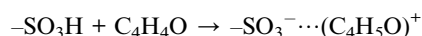
between these possibilities, we performed time dependent DFT calculations of geometry optimized protonated monomer and the partially protonated dimer and found the latter to agree more with the theoretical optical transitions.

On increased reaction time of furan/Nafion system the band at 290 nm grows and becomes clearly visible, this is representative of change of color of Nafion membrane from yellow (immediate after dosing furan Fig. 4(b) spectrum ii) to optical transitions further into the visible region with a yellow-brown color (after about 30 minutes contact time – spectrum e) assigned to C₁₂H₁₀O₃⁺ species (Scheme III†).

The band at ~437, ~465 and 550 nm becomes more clear upon heating the furan/Nafion system (at 100 °C) for 30 minutes causing change of color from yellow-brown to dark brown which can be attributed to the C₈H₉O₂⁺ carbocations³³ formed by proton assisted interaction of two furan molecules (Scheme II†). A broad band in region of 400 nm to 550 nm, corresponding to a neutral PT (polyfuran) state increased in intensity.³⁴

Furan/Nafion composite, immediately after sending of furan at room temperature (spectrum ii in Fig. 4(b)) this band is slightly perturbed with a slight shift to higher frequency. One can easily notice the weak band at approximately 232 nm associated with furan. With increasing contact time of furan/Nafion system, the band at *ca.* ~232 nm increases in intensity indicating the membrane soaked with furan; also appears band at 292 nm and weak absorptions in the region 322–555 nm.

The appearance of the band at 292 nm occurs in times comparable to those for the disappearance of the IR signals due to dissociated –SO₃H species and formation of charged conjugated species. This can then be ascribed to proton transfer from the protonated SO₃H in Nafion to the protonated monomer species formed by the following reaction:



This reaction is also supported by comparison with the IR spectra of the furan/Nafion system where one can note that the interaction of reaction products with the sulphonic groups can also give an explanation of the presence of large absorption in the infrared spectra covering the whole region between 3500 cm^{-1} and about 1600 cm^{-1} with presumable windows resonance at about 2240 and 1900 cm^{-1} .

After prolonged reaction time of furan/Nafion system with excess of furan at room temperature, formation of a complex broad and absorption in the region $434\text{--}303\text{ nm}$ and a band at 476 nm is observed, which further increases on heating treatment. By analogy with the cases discussed above we assign these absorptions to oligomeric species containing an increasing number of conjugated double bonds up to six units.

The rate of reaction of thiophene and furan is much higher in acidic medium as compared to that of pyrrole³⁵ due to this the dimeric and polymeric species formed at room temperature itself which is confirmed by the orange-brown color of the sample at RT. While in case of pyrrole the color appears comparatively faint at the beginning the reaction proceed more rapidly when the pyrrole/Nafion system kept allowed for longer reaction time in presence of excess pyrrole at room temperature, formation of tetramers confirmed by UV-visible spectra (Fig. 4(a) red spectrum e). The lower reactivity of successive oligomerization of the protonated pyrrole could here be understood by the much lower dimer dipole (1.94 D) compared to that of the protonated thiophene and furan dimers (4.24 D , and 3.25 D , respectively, see Table 2).

Experimental evidence for the presence of conjugated carbocationic species. The experimental and theoretical spectroscopic data are in very good agreement with the formation of conjugated carbocationic species containing an increasing number of conjugated double bonds. The presence of carbocationic species, however, can also be tested by dosing ammonia gas²⁸ Fig. 6.

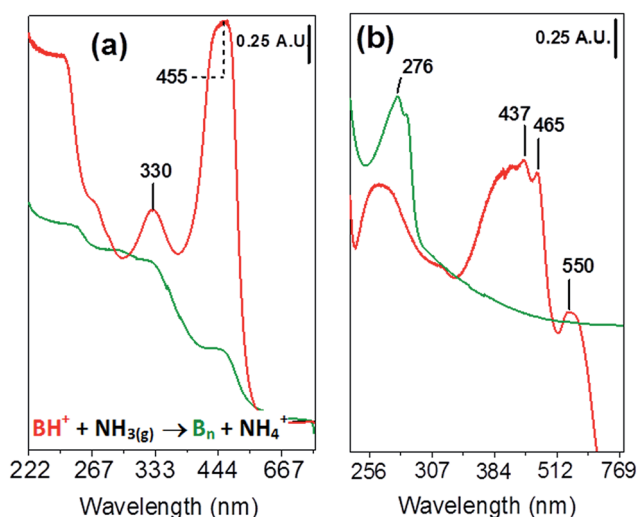
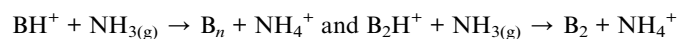


Fig. 6 UV-visible spectroscopy of pyrrole/Nafion (a), and thiophene/Nafion composite (b), red spectra represents respective composite sample after heat treatment at $100\text{ }^{\circ}\text{C}$ for 30 minutes, green spectra collected after 10 min of dosing $\text{NH}_3(\text{g})$ at room temperature.

It is here possible to study the interaction of colored species with ammonia and can be monitored by UV-Vis spectroscopy. The presence of $\text{NH}_3(\text{g})$ makes the transformation of highly colored oligomer into optically silent and neutral NH_4^+ . This is due to chemical reaction in contact with ammonia which removes a proton from the positively charged species forming ammonium ion and neutral molecules following the reaction scheme:



where, B and NH_3 represents Brønsted–Lowry acid and base respectively.

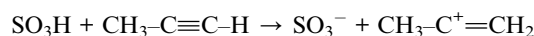
Since it is known that the carbocation species absorb at lower frequencies than its corresponding neutral species as shown previously,³⁶ the extraction of a proton must be accompanied by the weakening of the bands responsible for the coloration of the sample. The nature of the charge oligomers is demonstrated by the effect of dosage of base (ammonia) UV-visible spectrum. By introducing ammonia (Fig. S2(a) and (b),† spectrum b), in the pyrrole/Nafion and furan/Nafion system, the intense brown staining of the membrane weakens and erosion of the species characteristic of oligomer with bands at 423 and 500 nm (Fig. 6(a) and (b)).

For pyrrole/Nafion system the presence of conjugated carbocationic products is evident from the following observations; (i) upon $\text{NH}_3(\text{g})$ contact, the intense coloration of the samples fades. (ii) Bands at 250 to 277 nm is destroyed completely (the effect being partially reversible upon evacuation $\text{NH}_3(\text{g})$ at room temperature) shows that the dosage of $\text{NH}_3(\text{g})$ leads to the formation of NH_4^+ and to the erosion of the main bands attributed to the charged oligomeric species.

For furan/Nafion system the erosion of the bands characteristic of the oligomeric species (476 nm , $434\text{--}303\text{ nm}$) and monomer (243 nm) is observed and a new band at higher frequencies ($285\text{--}277\text{ nm}$) is also seen, likely to be from neutral species with a reduced degree of conjugation. Similar observations were noticed for the thiophene/Nafion system.

Oligomerisation of methyl-acetylene in Nafion membrane. As methyl-acetylene easily undergoes electrophilic addition reactions in the presence of Brønsted acid catalysts there is a potential to form carbocation species upon proton capture which in turn can enable an oligomerization reaction in similar way as the aromatic monomers.

Dosage of methyl-acetylene on Nafion results in the disappearance of the IR band at 910 cm^{-1} due to the $-\text{SO}_3\text{H}$ groups and in the appearance of that 1060 cm^{-1} due to the SO_3^- species. At the same time a band from the $\text{C}=\text{C}$ vibration (in positively charged species) is developed with time at 1680 cm^{-1} as shown in Fig. S3.† This behavior indicates the following reaction:



At this stage the membrane becomes pale orange in color and color intensifies on longer reaction or heating this reflects

formation of oligomers. This formation of oligomeric species can be well justified by the optical spectra (Fig. S3(c)†). Notice, that this reaction is also expected to destroy the UV-Vis band at 277 nm, which indeed is substituted by a new absorption nearly at the same position due to the $\text{CH}_3\text{-C}^+=\text{CH}_2$ species,¹⁹ further supporting the reaction above.

The chromophore responsible for the absorptions at 350 and 400 nm is more uncertain but can probably be associated with a sulphur-based group, and then more specifically with the chromophore containing $\cdot\text{SO}_3\text{H}$ radicals which eventually cleaves to produce SO_2 and a hydroxyl radical as end products and have been reported before in similar contexts.³³

Methyl-acetylene/Nafion system in presence of methyl-acetylene gas phase excess for a longer reaction time and thermal treatment, new bands develop at around 370 and 434 nm: these can be assigned to dimeric and trimeric charged oligomers, respectively, formed following the reaction sequence. The presence of two (in dimers) and three (in trimers) conjugated double bonds is responsible for the faint orange coloring of the membrane at room temperature.

Similar to the aromatic/Nafion system, the methyl-acetylene/Nafion composite shows formation of colored conjugated oligomers through formation of H-bonded carbocation adducts. On the basis of the vibrational spectra as well electronic vibration bands of the acetylenic compounds (including methyl-acetylene) in monomer form and in protonated form,³⁶ it is reasonable to assign these absorptions to the formation of oligomeric species. In particular, the band at around 370 nm is attributed to dimeric species $(\text{CH}_3\text{CCH})_2\text{H}^+$ and that to 434 nm trimeric species $(\text{CH}_3\text{CCH})_3\text{H}^+$, responsible for the pale orange color of the membrane. For the methylacetylene/Nafion system (alike that of pyrrol/Nafion and furan/Nafion system) heating does not substantially favor the formation of more conjugated products. The irreversible nature of species formed after protonation is shown by the fact that even after outgassing gas (spectrum 8 in Fig. S3(a) and (b)†), the $\nu(\text{C}=\text{C})$ stretching of the carbocations species (1680 cm^{-1}) remains, while bands due to methyl-acetylene gas phase; $2941\text{--}2881\text{ cm}^{-1}$ and 3008 cm^{-1} modes $\nu(\text{CH}_3)$, 3334 cm^{-1} mode $\nu(\text{CH})$ and 633 cm^{-1} $\delta(\text{CH})$ bending mode disappears.

In summary, the mechanism and progress of a controlled acid-catalyzed oligomerization *via* vapor pressure control of several classes of aromatic monomers (pyrrole, thiophene, and furan) and one unsaturated (methyl-acetylene) inside Nafion membranes are presented. The experimental IR and UV-Vis spectroscopy together with the theoretical assessments have allowed a detailed analysis of the intermediate species as well as products during the reaction. The three main parts of the activated proton transfer reaction and oligomerization can be summarized in the following (see also reaction Schemes I–III in Fig. S4, ESI†). First, contact with the reactants in gas form (pyrrole, thiophene, furan and methyl-acetylene) results in a transformation of hydrogen bonded species into positively charged oligomers through an activated proton transfer identified with IR spectroscopy. Subsequent heating ($\approx 100\text{ }^\circ\text{C}$) (with presence of excess of unsaturated species) favors the transformation of monomeric–dimeric carbocationic species into

respective carbocationic species (trimeric and tetrameric carbocationic species) *via* a dipole moment activated oligomerization where this in turn break the symmetry and IR activates the oligomerization bond in between the monomers. Longer reaction time or heating treatment with the presence of excess unsaturated or aromatic species favors the transformation of monomeric/dimeric carbocationic species into respective subsequent carbocationic species (trimeric/tetrameric carbocationic species) giving charged oligomers (Scheme III†). However, in case of pyrrol/Nafion system the formation of tetrameric oligomerization species takes place already at room temperature, Fig. 4(a)–(c) and 6(c).

Conclusions

An approach to perform controlled acid-catalyzed oligomerization *via* vapor pressure control of the reactions inside Nafion membranes is presented. FTIR data and UV visible spectroscopy supported by theoretical assignments reveal that the highly acidic Nafion membrane protonates aromatic pyrrole, thiophene, furan and methyl-acetylene to form a carbo-cationic polymeric chain at room temperature with the formation of hydrogen-bonded precursors. The H-bonded species is *via* IR spectroscopy seen to transform into positively charged oligomers through an activated proton transfer mechanism, a polymerization process that proceeds at room temperature with increased contact time with gas phase pyrrole, furan, thiophene and methyl-acetylene, respectively. The progress of the oligomerization process is also monitored at elevated temperature by analyzing the effective number of conjugated bonds *via* optical spectroscopy. The chemisorbed oligomeric-Nafion composite product formed are irreversible after complete outgassing the gas phase reactants and thus stable in ambient humidity, this is very important for practical application of the present route. The detailed study of the vibrational and optical transitions during the chemical polymerization mechanism presented here makes it possible to identify key intermediate species and add important information for control and monitoring of the oligomerization process for several classes of monomers. Our study shows a step forward both in the *in situ* preparation of conjugated hybrid Nafion membranes as well as insights into the details of the hybridization mechanism that open the possibility to control and utilize a larger set of hybridization approaches for improved efficiency and stability of these materials.

Author contributions

S. M. J. evolved the idea through experiments, prepared Nafion membranes for characterization, performed dosing of heterocycles (pyrrol, furan, thiophene) and unsaturated (methyl-acetylene) gas phase molecules, carried out FTIR, UV-visible measurements, data plotting as well analysis and writing of the manuscript; S. T. participated in preparation of Nafion membranes and analysis of materials; S. T. participated editing of the manuscript, G. S. partially participated in the project, T. E. performed DFT calculations, analysis and participated in

writing, assisted in plotting data and performed final editing of the manuscript.

Acknowledgements

The Uppsala Multidisciplinary Center for Advanced Computational Science (UPPMAX) is acknowledged for providing computational resources under projects snic 2015-6-83 and snic 2015-1-281.

Notes and references

- W. G. F. Grot, V. Mehra, G. E. Munn and J. C. Solenberger, *J. Electrochem. Soc.*, 1975, **122**, C104.
- H. S. White, J. Leddy and A. J. Bard, *J. Am. Chem. Soc.*, 1982, **104**, 4811–4817.
- K. A. Mauritz and R. B. Moore, *Chem. Rev.*, 2004, **104**, 4535–4585.
- K. S. Rohr and Q. Chen, *Nat. Mater.*, 2008, **7**, 75–83.
- H. Itoa, T. Maeda, A. Nakano and H. Takenaka, *Int. J. Hydrogen Energy*, 2011, **36**, 10527–10540.
- R. Kannan, B. A. Kakade and V. K. Pillai, *Angew. Chem., Int. Ed.*, 2008, **47**, 2653–2656.
- P. Sridhar, R. Perumal, N. Rajalakshmi, M. Raja and K. S. Dhathathreyan, *J. Power Sources*, 2001, **101**, 72–78.
- S. Staschewski, *Int. J. Hydrogen Energy*, 1996, **21**, 381–385.
- M. Han, S. H. Chan and S. P. Jiang, *Int. J. Hydrogen Energy*, 2007, **32**, 385–391.
- F. N. Büchi and S. Srinivasan, *J. Electrochem. Soc.*, 1997, **144**, 2767–2772.
- D. C. Lee, H. N. Yang, S. H. Park and W. J. Kim, *J. Membr. Sci.*, 2014, **15**, 20–28.
- B. Schwenzer, S. Kim, M. Vijayakumar, Z. Yang and J. Liu, *J. Membr. Sci.*, 2011, **372**, 11–19.
- H. S. Park, Y. J. Kim and W. H. Lee, *J. Membr. Sci.*, 2006, **272**, 28–30.
- N. Jia, M. C. Lefebvre, J. Halfyard, Z. Qi and P. C. Pickup, *Electrochem. Solid-State Lett.*, 2000, **3**, 529–531.
- M. Malinowski, A. Iwan, K. Parafiniuk, L. Gorecki and G. Pasciak, *Int. J. Hydrogen Energy*, 2015, **40**, 833–840.
- A. Iwan, M. Malinowski, A. Sikora, I. Tazbir and G. Pasciak, *Electrochim. Acta*, 2015, **164**, 143–153.
- K. Feng, L. Liu, B. Tang, N. Li and P. Wu, *ACS Appl. Mater. Interfaces*, 2016, **8**, 11516–11525.
- M. Hiza, H. Hasegawa and T. Higashimura, *Polym. J.*, 1980, **12**, 379–385.
- A. Zecchina, G. Spoto and S. Bordiga, *Phys. Chem. Chem. Phys.*, 2005, **7**, 1627–1642.
- R. Buzzoni, S. Bordiga, G. Ricchiardi, G. Spoto and A. Zecchina, *J. Phys. Chem.*, 1995, **99**, 11937–11951.
- M. J. Frisch, G. W. Trucks, H. B. Schlegel, G. E. Scuseria, M. A. Robb, J. R. Cheeseman, G. Scalmani, V. Barone, B. Mennucci, G. A. Petersson, H. Nakatsuji, M. Caricato, X. Li, H. P. Hratchian, A. F. Izmaylov, J. Bloino, G. Zheng, J. L. Sonnenberg, M. Hada, M. Ehara, K. Toyota, R. Fukuda, J. Hasegawa, M. Ishida, T. Nakajima, Y. Honda, O. Kitao, H. Nakai, T. Vreven, J. A. Montgomery Jr, J. E. Peralta, F. Ogliaro, M. Bearpark, J. J. Heyd, E. Brothers, K. N. Kudin, V. N. Staroverov, R. Kobayashi, J. Normand, K. Raghavachari, A. Rendell, J. C. Burant, S. S. Iyengar, J. Tomasi, M. Cossi, N. Rega, J. M. Millam, M. Klene, J. E. Knox, J. B. Cross, V. Bakken, C. Adamo, J. Jaramillo, R. Gomperts, R. E. Stratmann, O. Yazyev, A. J. Austin, R. Cammi, C. Pomelli, J. W. Ochterski, R. L. Martin, K. Morokuma, V. G. Zakrzewski, G. A. Voth, P. Salvador, J. J. Dannenberg, S. Dapprich, A. D. Daniels, Ö. Farkas, J. B. Foresman, J. V. Ortiz, J. Cioslowski and D. J. Fox, *Gaussian 09, Revision A.01*, Gaussian, Inc., Wallingford CT, 2009.
- W. J. Feast, J. Tsibouklis, K. L. Pouwer, L. Groenendal and E. W. Meijer, *Polymer*, 1996, **37**, 5017–5047.
- S. Sadki, P. Schottland, N. Brodie and G. Sabouraud, *Chem. Soc. Rev.*, 2000, **29**, 283–293.
- R. Becker, C. Sigwart, M. Hesse, R. Fischer, K. Eller, G. Heilen and K.-D. Plitzko, *US Pat.*, 5,773,648, June 30 1998.
- J. Doan, N. E. Navarro, D. Kumari, K. Anderson, E. Kingston, C. Johnson, A. Vong, N. Dimakis and E. S. Smotkin, *Polymer*, 2015, **73**, 34–41.
- E. L. Varetti, *Spectrochim. Acta*, 1988, **44**, 733–738.
- P. S. Gejji, K. Hermansson and J. Lindgren, *J. Phys. Chem.*, 1993, **97**, 3712–3715.
- G. Spoto, F. Geobaldo, S. Bordiga, C. Lamberti, D. Scarano and A. Zecchina, *Top. Catal.*, 1999, **8**, 279–292.
- C. L. Garcia and J. A. Lercher, *J. Phys. Chem.*, 1992, **96**, 2669–2675.
- M. E. Nicho, H. Hu, M. Lopez and C. J. Escalante, *Sol. Energy Mater. Sol. Cells*, 2004, **82**, 105–118.
- E. Ando, S. Onodera, M. Iino and O. Ito, *Carbon*, 2001, **39**, 101–108.
- G. A. Arbuckle, A. G. MacDiarmid, S. Lefrant, T. Verdon, E. Mulazzi, G. P. Brivio, X. Q. Yang, H. S. Woo and D. B. Tanner, *Phys. Rev. B: Condens. Matter Mater. Phys.*, 1991, **43**, 4739–4747.
- C. A. Wilkie, J. R. Thomsen and M. L. Mittleman, *J. Appl. Polym. Sci.*, 1991, **42**, 901–909.
- F. Geobaldo, G. T. Palomino, S. Bordiga, A. Zecchina and C. O. Arean, *Phys. Chem. Chem. Phys.*, 1999, **1**, 561–569.
- R. F. Curtis, D. M. Jones and W. A. Thomas, *J. Chem. Soc. C*, 1971, 234–238.
- S. Bordiga, G. Ricchiardi, G. Spoto, D. Scarano, L. Carnelli, A. Zecchina and O. C. Arean, *J. Chem. Soc., Faraday Trans.*, 1993, **89**, 1843–1855.